DOI: 10.1021/ma101533f

Macromolecules
ARTICLE

EPR Simulation of Polyenyl Radicals in Ultrahigh Molecular Weight Polyethylene

Michael J. Kasser, Joseph Silverman, and Mohamad Al-Sheikhly*

Department of Materials Science and Engineering, University of Maryland, College Park, Maryland 20742

Received July 8, 2010; Revised Manuscript Received September 7, 2010

ABSTRACT: An irradiated polyethylene sample containing mostly dienyl free radicals was fabricated by using a combination of photo and thermal treatments. This allowed, for the first time, unambiguous observation of the dienyl radical's EPR signal to be a singlet with eight hyperfine peaks 9 G apart. Accurate simulation parameters for the dienyl radical were determined. While inaccurate for the dienyl radical, the assumption that a smooth singlet can simulate polyenyl radicals holds true for higher-order polyenyl radicals. The line width of the polyenyl singlet is a function of the radical's location, with the line width decreasing as the surrounding morphology becomes more organized and uniform, as is the case in the crystalline region. The decreasing line width of polyenyl spectra after exposure to air suggests that the rate of oxidatively induced crystallization is more rapid than oxygen diffusion within the polymer.

Introduction

Despite its simple chemical structure, the radiation chemistry of polyethylene is a complex problem, and several different types of free radicals, including the alkyl, allyl, and polyenyl radicals, are generated by ionizing radiation. Electron paramagnetic resonance spectroscopy (EPR) is a powerful characterization technique used to investigate free radicals. However, irradiated polyethylene contains various combinations of free radicals, depending on dose, thermal history, environment, and sample morphology. Since the spectra of the different radicals overlap, the experimentally observed spectra are quite complex. Attempts to examine only one species, or a ratio of species, from such spectra have included power saturation techniques,[1−3] differing radiation doses,[4] differing spectra widths,[5,6] and relative peak heights.[7] Currently, the most accurate way to interpret complex spectra involves simulating them, which requires *a priori* knowledge of each radical's relative concentration, hyperfine constants, and line widths. Most often, educated guesses resulting in best fits are made for these parameters, since, aside from alkyl radicals at low temperature, individual species cannot be examined. Therefore, *a priori* knowledge of the hyperfine constants and line widths of other radicals present in irradiated polyethylene would improve the ability to simulate complex spectra.

Of all the radicals, the spectrum of the alkyl radical is best known. It consists of a symmetrical sextet and is accurately simulated via the hyperfine separation constants $H_\alpha \sim 22$ G and $H_\beta \sim 33$ G. The line width of the peaks depends on the variation in the distance between the unpaired electron and nearby unpaired protons and, hence, is a function of radical location and sample morphology.[8] The alkyl spectrum is well-known because it is simple to create a polyethylene sample containing only alkyl-free radicals by irradiating at liquid nitrogen temperatures. The spectrum of the allyl radical is not as well-known. While it is accepted to consist of a septet superimposed on a broad singlet, there is a good deal of discrepancy in the literature about its hyperfine separation and proper simulation parameters[2,9−15] since they often depend on variables such as instrument settings and sample morphology. While polyenyl radicals are a family of free radicals, i.e., dienyl, trienyl, tetraenyl, etc., they are often lumped together since it is believed that their EPR spectra is a simple singlet. The loss of hyperfine structure is not due to lack of interacting hydrogen atoms, but to the inability of the EPR to resolve the narrowing hyperfine separation.[4] However, more accurate spectra simulations have been achieved by assuming that the dienyl and trienyl free radical possess some hyperfine structure.[2] It is also believed that the singlet's line width decreases with increasing unsaturation.[4]

Experimental Section

Methods. Medical grade UHMWPE (GUR 1050) was microtomed into 200 μm films then placed in EPR tubes and irradiated with a 7 MeV electron-beam to a dose of 100 kGy in a nitrogen environment. In this work, "UV films" are electron-beam irradiated films that were subsequently annealed at 100 °C for 2 h, then photoirradiated with a 325 W short arc xenon lamp (Schoeffel Instruments Corp., Westwood, NJ) at a distance of 44 cm for 1 h, and annealed again at 100 °C for 2 h. This process was repeated three times for a total of 8 h of annealing and 3 h of photoirradiation. "Control films" are electron-beam irradiated films that received identical thermal treatments, but no photo-treatments. The xenon lamp emits a continuous spectrum from 200 nm to the IR region, and the lamp's output between 300 and 390 nm at 44 cm was measured (Blak-Ray Model J221, Upland, CA) to be 5200 ± 340 μW/cm^2. The entire film fabrication was performed in a nitrogen environment. EPR spectra were recorded throughout sample fabrication and the UV−vis spectra were recorded at the conclusion of all treatments. After fabrication, the films were exposed to air at room temperature. The evolution of the EPR and UV−vis spectra was recorded for up to 800 h.

In order to investigate the effect of prolonged photoirradiation, a film was electron-beam irradiated to 100 kGy and then continuously photoirradiated for 10 h. The EPR and UV spectra were recorded at various times throughout the experiment. Film fabrication and all measurements were performed in a nitrogen environment.

Measurement and Characterization. All EPR measurements were performed using an ESP300 spectrometer (Bruker Biospin, Billerica, MA) with the following instrument parameters: microwave

*Corresponding author. E-mail: mohamad@umd.edu.

 Published on Web 10/08/2010

Table 1. UV Absorption Maxima for Conjugated Unsaturations and Free Radicals in Polyethylene[16]

unsaturation	wavelength, nm	free radical	wavelength, nm
diene	235	allyl	258
triene	275	dienyl	285
tetraene	310	trienyl	323
pentaene	340	tetraenyl	359
		pentaenyl	396

frequency of 9.42 GHz, microwave power of 0.5 mW, frequency modulation of 100 kHz, modulation amplitude of 6.23 G, receiver gain of 50 000, center field at 3350 G, sweep width of 300 G, conversion time of 2.54 ms, and time constant of 2.54 ms. It was verified that the modulation amplitude, as well as the ratio of the conversion time to time constant, did not distort the signal. While the alkyl radical's signal is slightly power-saturated at 0.5 mW, this power was used due to improvement in signal quality. A total of 30 scans were added to improve the signal-to-noise ratio.

All UV−vis measurements were made using a Cary-3 spectrophotometer (Varian, Palo Alto, CA) between 200 to 550 nm. A film holder was modified by inserting a piece of aluminized polyethylene containing a slit that was slightly smaller than the UHMWPE films being measured, ensuring that light was transmitted only through the films. For measurements in an air environment, films of comparable thickness were inserted into both the measurement and reference beam. For measurements in a nitrogen environment, the sample film was loaded into a nitrogen-filled glovebox, placed in a film holder which was machined to fit in a quartz cuvette, and sealed with a rubber stopper. The reference sample was contained in a similar film holder in a quartz cuvette, but was exposed to air. A table listing relevant absorption maxima for unsaturations and free radicals can be seen in Table 1.

Results and Discussion

The Dienyl Radical EPR Spectrum. The change in EPR spectrum of the non-UV control film is shown in Figure 1, while the change in EPR spectrum of the UV film is shown in Figure 2. For both samples, the initial, six-peaked, mostly alkyl spectrum decays to a five-peaked spectrum. This spectrum corresponds to the five strongest peaks of the allyl free radical, with a small contribution from polyenyl radicals. In the control film, all of the peaks continue to decay evenly with increasing annealing time. In contrast, the allyl spectrum of the UV film is converted to a six-peaked, mostly alkyl spectrum. This change is due to photoconversion of allyl radicals to alkyl radicals.[6,17] Subsequent thermal treatment results in a singlet containing at least six hyperfine peaks about 9 G apart. This is an unusual spectrum and has not previously been assigned in polyethylene. Subsequent photo- and thermal treatments do not significantly alter the spectra, although overall peak height and hyperfine peak heights are reduced. The 9 G hyperfine separation is too small to be attributed to the allyl radical whose separation is reported between 12 and 18 G.[18,19] This structure also cannot be attributed to some combination of the alkyl and allyl free radicals since, after thermal treatment, there are virtually no alkyl radicals present. It also cannot be attributed to a peroxyl free radical because it power-saturates[3] and does not change upon cooling to −163 °C.[11,20]

UV spectroscopy is another useful method to identify free radicals in polyethylene.[16,21] A comparison of the UV spectra of the control and UV films is shown in Figure 3. From the similar peak at 235 nm, it is clear that the films contain a comparable concentration of dienes. However, the presence of a shoulder at 258 nm for the control film shows that it contains more allyl radical than the UV film. Conversely, the much larger peak at 285 nm for the UV film indicates that it contains more of the dienyl radical than the control film. The UV film also has a very weak absorbance at 323 nm, indicating the presence of a small amount of trienyl radicals. These absorptions suggest that the singlet with 9 G hyperfine separation should be attributed to the dienyl radical. Spectral simulations below confirm this assignment.

A schematic drawing of the dienyl free radical is shown in Figure 4. Because of resonance stabilization, the unpaired electron is distributed over five carbon atoms. Various

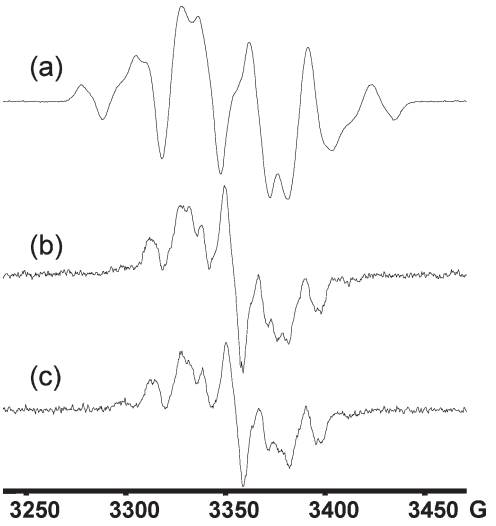

Figure 1. EPR spectra of the control film after (a) irradiation to 100 kGy, (b) a subsequent 2 h anneal at 100 °C, and (c) another 2 h anneal at 100 °C. Part a mostly consists of a sextet corresponding to the alkyl radical while parts b and c are a pentet, likely corresponding to the five strongest peaks of the allyl radical. Note that the vertical scale is reduced by a factor of 5 in part a.

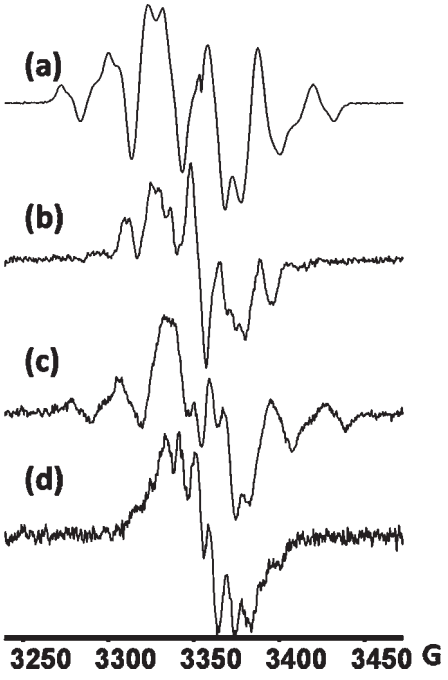

Figure 2. EPR spectra of the UV film after (a) irradiation to 100 kGy, (b) a subsequent 2 h anneal at 100 °C, (c) a subsequent 1 h photoirradiation and (d) a subsequent 2 h anneal at 100 °C. Part d is an unusual spectrum consisting of a singlet with six hyperfine peaks 9 G apart. The vertical scale in part a is reduced by a factor of 10 while parts b and c are reduced by as factor of 2.

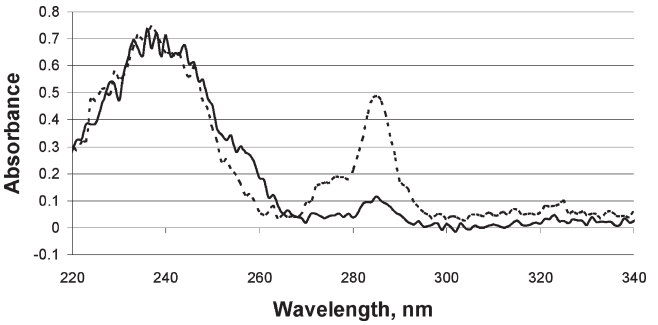

Figure 3. UV spectra of the control film after an 8 h anneal at 100 °C (solid line) and of the UV film after sequential 2 h, 100 °C anneals, and 1 h phototreatments, totaling 3 h of photoirradiation and 8 h of thermal annealing (dotted line). The UV film contains less allyl and more dienyl radicals than the control film.

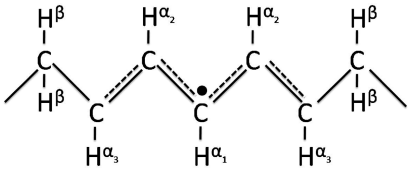

Figure 4. Schematic diagram of the dienyl free radical. The unpaired electron is stabilized over five carbon atoms.

calculations have shown that while the electron density is symmetrical about the central carbon, it varies for different carbons.[22] It is therefore reasonable to assume that there are three different α protons. It is also reasonable to assume that there are four identical β protons adjacent to the free radical. On the basis of these assumptions, the dienyl radical was accurately simulated using WINSIM[2] (Figure 5) and the simulation parameters are summarized in Table 2. The uncertainties listed in the table are the standard deviation of the results from all simulations whose correlation factor (a measure of how accurately the simulation matches the experimental spectrum) is greater than 98%. The average correlation for all considered simulations is 98.7%. Simulations were performed for only dienyl radical spectra immediately following a UV treatment, when it is reasonable to assume that only alkyl and polyenyl, but no allyl, radicals are present. These spectra were chosen over those possibly containing allyl radicals since the simulation parameters are well-known for the alkyl, but not the allyl, radical. It is worthwhile to note that the hyperfine coupling constants for the α_2 and α_3 protons are quite close and the spectra can be accurately simulated by assuming one α_1 and four α_2 protons.

Higher-Order Polyenyl Radicals. In order to investigate the spectra of higher-order polyenyl radicals, a longer, continuous photoirradiation was performed. The EPR and UV spectra as a function of photoirradiation time in a nitrogen environment are shown in Figure 6. The initial EPR spectrum consists of mostly alkyl radicals, although, from the UV spectrum, some allyl and dienyl radicals are also present. After 2 h of photoirradiation, a singlet with 9 G hyperfine separation, consisting of mostly dienyl and trienyl radicals, is observed. As the dienyl radical concentration decreases, the hyperfine structure is lost and, after 10 h, only a smooth singlet remains. This corresponds to a consumption of lower-order radicals and an increase in higher-order free radicals. The mechanism for the photoconversion of lower-order polyenyl radicals to higher-order polyenyl radicals is beyond the scope of this article, and is discussed elsewhere.[23] It is noteworthy that, contrary to previous reports,[4] the line width of the singlet does not decrease as the degree of conjugation increases. The cause of the sharpening of the polyenyl singlet is discussed below.

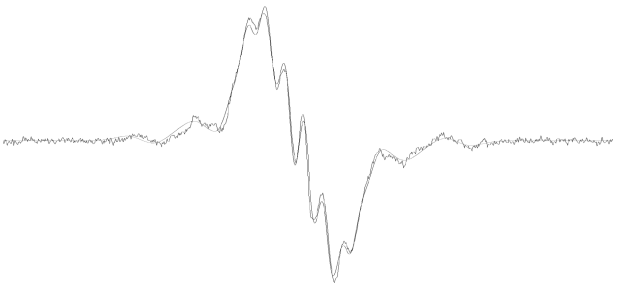

Figure 5. Simulation of the experimentally observed dienyl radical. The darker, noisier experimental spectrum is overlaid on the lighter, smooth simulation spectra. The simulated spectrum is a combination of an alkyl sextet and a singlet with 9 G hyperfine separation assigned to the dienyl radical.

Table 2. Simulation Parameters for the Alkyl, Dienyl, and Polyenyl Radicals[a]

radical	line width, G	$H_{\alpha 1}$, G	$H_{\alpha 2}$, G	$H_{\alpha 3}$, G	H_{β}, G
alkyl	8.4 ± 0.6	23.6 ± 1.4	N/A	N/A	30.7 ± 0.3
dienyl	5.4 ± 0.2	9.6 ± 1.3	8.3 ± 0.7	8.1 ± 0.4	10.2 ± 0.3
polyenyl	14.5 ± 0.4				

[a] There is one α proton and four β protons for the alkyl radical and one α_1 proton, two α_2 and α_3 protons, and four β protons for the dienyl radical. The polyenyl radical can be simulated as a smooth singlet without hyperfine structure.

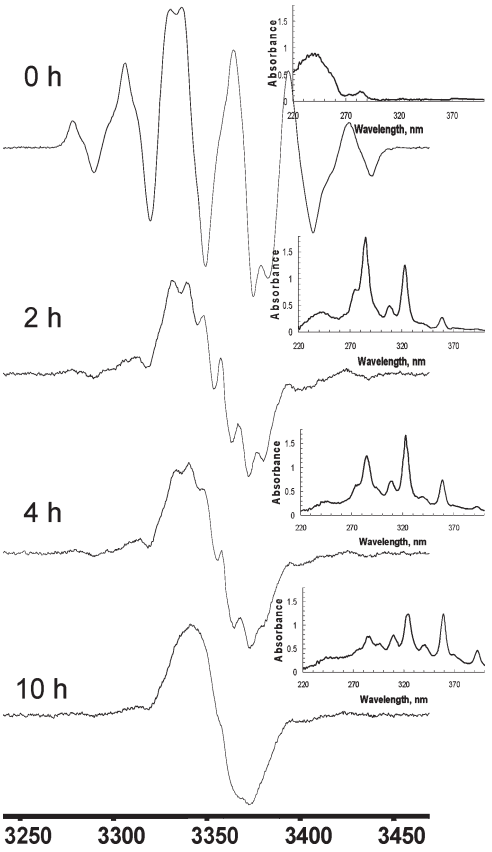

Figure 6. EPR and UV spectra (inset) of an electron-beam irradiated UHMWPE film upon increasing photoirradiation. With increasing photoirradiation, the hyperfine structure of the EPR spectra is lost, although the line width of the singlet does not decrease. From the UV spectra, it is clear this corresponds to the consumption of lower-order free radicals and creation of higher-order radicals.

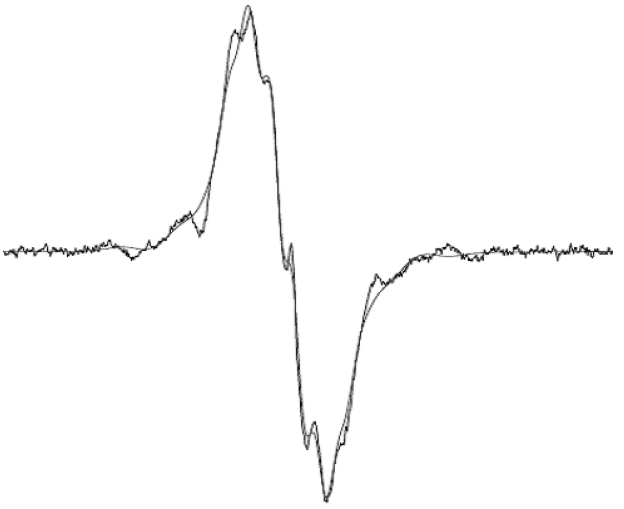

Figure 7. Simulation of the EPR spectrum observed after 6 h of photoirradiation in a nitrogen environment. The darker, noisier experimental spectrum is overlaid on the lighter, smooth simulation spectra. Simulated spectrum is a combination of alkyl, dienyl, and smooth singlet approximating higher-order polyenyl radicals. The relative concentration of each species is shown in Figure 8.

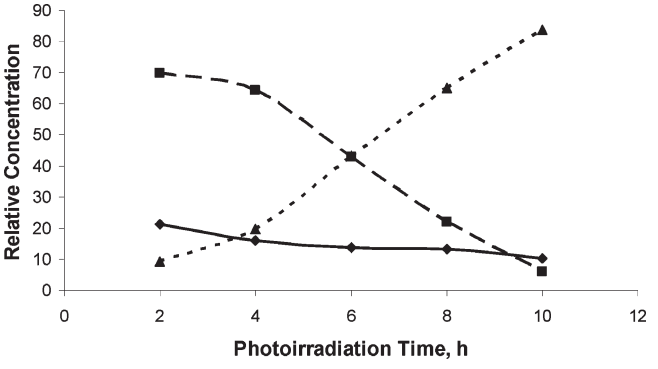

Figure 8. Relative concentration of alkyl (solid line), dienyl (dashed line), and polyenyl (dotted line) radicals with increasing photoirradiation time, as determined by EPR spectral simulation. From 2 to 10 h of photoirradiation, the relative concentration of alkyl radicals slowly decreases, the dienyl concentration sharply decreases, and the polyenyl concentration sharply increases. It was not possible to accurately simulate shorter photoirradiation times due to the presence of allyl radicals.

Using the simulation parameters for the alkyl and dienyl radicals, it is possible to simulate the EPR spectra of the continuously photoirradiated film by adding a smooth singlet, see Table 2. The smooth singlet is an adequate approximation of higher-order polyenyl (trienyl and higher) radicals which either lack or contain only subtle hyperfine structure. An example of a simulated spectrum is shown in Figure 7. The change in relative concentration of the alkyl, dienyl, and polyenyl radicals with increasing photoirradiation time, as determined by spectral simulation, is shown in Figure 8. While the relative concentration of alkyl radicals only slowly decreases with increasing photoirradiation, the dienyl concentration sharply decreases and the polyenyl concentration sharply increases. A similar progression is evident from the UV spectra in Figure 7, supporting EPR simulation results. Unfortunately, a more rigorous comparison between EPR and UV−vis results is not possible as polyenyl radical concentrations cannot be accurately determined since polyenyl radical molar absorptivities are unknown.

The Sharp, Oxidation-Induced Singlet. The changes in EPR spectra upon increasing exposure time to air at room temperature for the control and UV film are shown in Figure 9 and Figure 10, respectively. Despite having different initial free radical species and concentrations, both films have a similar spectral progression. After exposure to air for 200 h, a combination of a singlet and a pentet is clearly visible. Upon further exposure to air, the pentet decays and only a sharp singlet remains. This decay occurs more quickly in the UV film as compared to the control.

The five peaks of the pentet are approximately 20 G apart and likely correspond to the five strongest peaks of the allyl free radical.[24,25] Allyl radicals are formed during the oxidation of polyethylene via the abstraction of allylic hydrogen

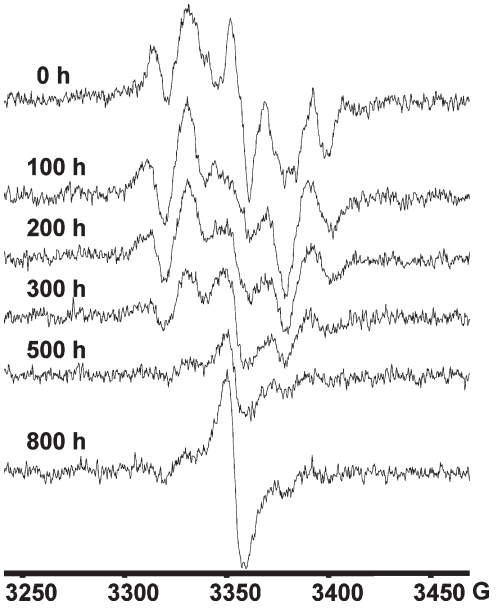

Figure 9. EPR spectral evolution with exposure time to air at room temperature of the control film that was annealed at 100 °C for 8 h. The initial, mostly allyl spectrum decays and is replaced with a sharp singlet that is attributed to a polyenyl radical trapped in the crystalline region formed by oxidative chain scission. The vertical scale for all spectra in Figure 9 and 10 are identical.

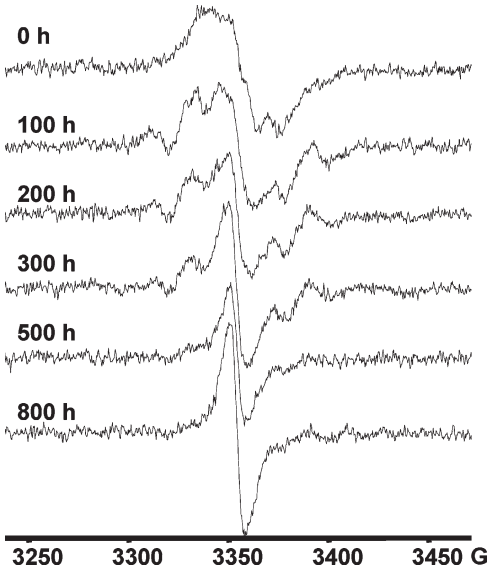

Figure 10. EPR spectral evolution with exposure time to air at room temperature of the UV film. The initial, mostly polyenyl spectrum decays into a combination of a five-peaked allyl spectrum and a sharp singlet. With increasing exposure time, the allyl component decays while the sharp singlet increases.

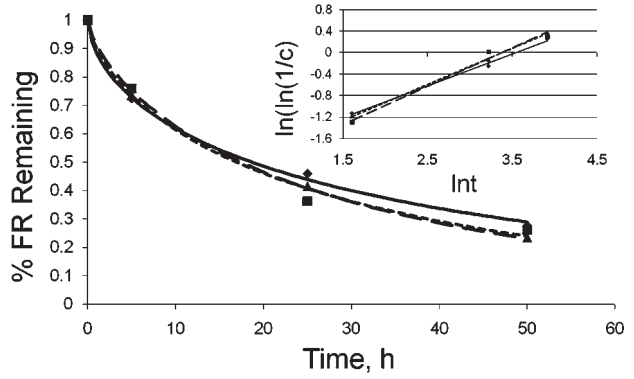

Figure 11. Concentration of dienyl (diamonds, solid line), trienyl (squares, dashed line), and tetraenyl (triangle, dotted line) upon increasing exposure time to air as measured by change in UV spectra peak height. Points represent an average of three samples. Inset shows a linear plot of $\ln(t)$ versus $\ln(\ln(1/C))$, where C is the relative concentration, showing an excellent fit with dispersive first order decay. Results from the inset are used to plot the decay curves in the main graph.

by the peroxyl radical. Allylic hydrogens are preferentially abstracted due to their lower bond energies (12 kcal/mol[26]) as compared to saturated hydrocarbons.

The assignment of the sharp singlet is not obvious. At least two types of free radicals are known to exhibit singlet spectra in polyethylene, the peroxyl and polyenyl free radicals. Power saturation experiments reveal that the sharp singlet power saturates and cannot be assigned to the peroxyl free radical.[3] Therefore, the radical is most likely a polyenyl radical. Polyenyl radicals can be created during the oxidation of polyethylene by the abstraction of allylic hydrogen of a conjugated unsaturation by a peroxyl radical. These hydrogens have significantly lower bond energies (> 19 kcal/mol[26]) than saturated hydrocarbons. Since photoirradiated films contain a higher concentration of conjugated unsaturations, the sharp singlet is formed more quickly and to a greater extent in those films.

There are two difficulties with this assignment. It is surprising that the polyenyl radicals are stable in the presence of oxygen since it is clear from Figure 10 that polyenyl radicals are transformed into peroxyl radicals in the presence of oxygen. However, polyenyl radicals can only combine with oxygen if they have access to it. Oxygen cannot enter the crystalline region.[27] It is also known that oxidation increases crystallinity via oxidative chain scission which allows previously constrained chains to fold into new crystals.[28] Therefore, it is possible that these radicals become trapped in the newly formed crystals and are no longer accessible to oxygen. Since the solubility of oxygen in crystalline UHMWPE is negligible, these results suggest that the rate of formation of a protective crystal structure around the newly formed radical site is more rapid than the transport of diffused oxygen to that site.

It is also surprising that the final polyenyl radical spectrum is considerably sharper than the initial polyenyl radical spectrum (compare spectra at 0 and 800 h in Figure 10). This effect has been reported by others[3] and has been attributed to the selective oxidation of lower-order polyenyl radicals, based on the assumption that lower-order polyenyl radicals are more reactive and have larger line widths. However, Figure 6 shows that different polyenyl radicals have identical line widths. Additionally, it is shown in the next section that all polyenyl radicals oxidize at a similar rate. Rather, the sharper line width is likely due to the radicals being located in the crystalline region. Line width broadening is due to variations in the distance between the free radical and neighboring protons. In the crystalline region, chains are held more rigidly in place and there is less variation. This effect has previously been used to explain the sharpening of an alkyl radical EPR signal in polyethylene.[8]

Oxidative Decay of Polyenyl Radicals. Upon exposure to air, polyenyl radicals decay by a combination of two steps: diffusion of oxygen to the radical site and the formation of the peroxyl radical. The oxidative decay of various polyenyl radicals is shown in Figure 11. Only samples and exposure times ($\leq$ 50 h) containing an adequate amount of free radicals to allow accurate measurement are included. The oxidative decay rate of all polyenyl radicals is nearly identical and is best described by dispersive first-order kinetics[29] (inset of Figure 11). The fact that all polyenyl radicals decay at the same rate demonstrates that the rate-limiting step is the diffusion of oxygen to the radical site. There is a variation in the nature of the radical sites and the difficulty of oxygen to access and react with them. This gives rise to our use of dispersive, first- order kinetics for polyenyl radical decay in which a time-dependent reaction constant is used to account for reaction rate dependence of oxygen diffusion to sites that are increasingly harder to reach.

Conclusions

The results and methods presented in this article provide a significant improvement in the accuracy of EPR simulation of radical species present in irradiated polyethylene. The EPR spectrum of the dienyl radical has been isolated and accurate simulation parameters have been determined. Additionally, it has been verified that a simple singlet can simulate higher-order polyenyls, but that the line width of the singlet depends on radical location. Further experiments are required to fully investigate the effect of sample morphology, temperature, and instrument parameters on the polyenyl radical EPR spectra. Improved ability to simulate spectra may result in improved understanding of the radiation chemistry of polyethylene and its application to the technology of UHMWPE implants.

Additional insight into the oxidation of UHMWPE has also been gained. All polyenyl radicals oxidatively decay at the same rate as the decay is limited by the diffusion of oxygen to the radical site. Resultant peroxyl radicals preferentially abstract hydrogens from the allylic sites of unsaturations due to lower bond energies. Additionally, the presence of polyenyl radicals in the newly formed, oxygen- induced crystals suggest that the rate of crystal formation is greater than the diffusion rate of oxygen in UHMWPE.

We thank Biomet for its generous gift of machined medical grade UHMWPE.

References and Notes

(1) Jahan, M. S.; Durant, J. *Nucl. Instrum. Methods Phys. Res., Sect. B: Beam Interact. Mater. At.* **2005**, *236*, 166–171.
(2) Durant, J.; Jahan, M. S. *Nucl. Instrum. Methods Phys. Res., Sect. B: Beam Interact. Mater. At.* **2005**, *236*, 160–165.
(3) Ohnishi, S. I.; Sugimoto, S. I.; Nitta, I. *J. Polym. Sci., Part A: Gen. Pap.* **1963**, *1* (2), 605–622.
(4) Ohnishi, S. I.; Ikeda, Y.; Sugimoto, S. I.; Nitta, I. *J. Polym. Sci.* **1960**, *47* (0149), 503–507.
(5) Johnson, D. R.; Wen, W. Y.; Dole, M. *J. Phys. Chem.* **1973**, *77*, 2174–2179.
(6) Waterman, D. C.; Dole, M. *J. Phys. Chem.* **1970**, *74*, 1913–1922.
(7) Auerbach, I. *Polymer* (*England*) **1966**, *7*, 283–92.
(8) Shimada, S.; Maeda, M.; Hori, Y.; Kashiwabara, H. *Polymer* **1977**, *18* (1), 19–24.
(9) Kuzuya, M.; Kondo, S.; Sugito, M.; Yamashiro, T. *Macromolecules* **1998**, *31* (10), 3230–3234.
(10) Naheed, N.; Jahan, M. S.; Ridley, M. *Nucl. Instrum. Methods Phys. Res., Sect. B: Beam Interact. Mater. At.* **2003**, *208*, 204–209.

(11) O'Neill, P.; Birkinshaw, C.; Leahy, J. J.; Barklie, R. *Polym. Degrad. Stab.* **1999**, *63* (1), 31–39.
(12) Alam, T. M.; Celina, M.; Collier, J. P.; Currier, B. H.; Currier, J. H.; Jackson, S. K.; Kuethe, D. O.; Timmins, G. S. *J. Polym. Sci., Part A: Polym. Chem.* **2004**, *42*, 5929–5941.
(13) Assink, R. A.; Celina, M.; Dunbar, T. D.; Alam, T. M.; Clough, R. L.; Gillen, K. T. *Macromolecules* **2000**, *33*, 4023–4029.
(14) Jahan, M. S.; Fuzail, M. *Nucl. Instrum. Methods Phys. Res., Sect. B: Beam Interact. Mater. At.* **2007**, *265*, 67–71.
(15) Jahan, M. S.; Stovall, J. C.; King, M. C. *Nucl. Instrum. Methods Phys. Res., Sect. B: Beam Interact. Mater. At.* **2001**, *185*, 323–327.
(16) Waterman, D. C.; Dole, M. *J. Phys. Chem.* **1970**, *74*, 1906–1912.
(17) Ohnishi, S. I.; Nitta, I.; Sugimoto, S. I. *J. Chem. Phys.* **1963**, *39*, 2647–2653.
(18) Jahan, M. S.; McKinny, K. S. *Nucl. Instrum. Methods Phys. Res., Sect. B: Beam Interact. Mater. At.* **1999**, *151*, 207–212.
(19) Ohnishi, S.; Ikeda, Y.; Kashiwagi, M.; Nitta, I. *Polymer* **1961**, *2*, 119–141.
(20) Hori, Y.; Shimada, S.; Kashiwabara, H. *Polymer* **1977**, *18*, 1143–1148.
(21) Bodily, D. M.; Dole, M. *J. Chem. Phys.* **1966**, *45*, 1428–1432.
(22) Bally, T.; Hrovat, D. A.; Borden, W. T. *Phys. Chem. Chem. Phys.* **2000**, *2*, 3363–3371.
(23) Kasser, M. J.; Silverman, J.; Al-Sheikhly, M. *Macromolecules* **2010**, in press; DOI: 10.1021/ma101532t.
(24) Ohnishi, S.; Sugimoto, S.; Nitta, I. *J. Chem. Phys.* **1962**, *37*, 1283–1288.
(25) Charlesby, A.; Libby, D.; Ormerod, M. G. *Proc, R, Soc, London, Ser. A: Math. Phys. Sci.* **1961**, *262* (1309), 207–218.
(26) McMillen, D. F.; Golden, D. M. *Annu. Rev. Phys. Chem.* **1982**, *33*, 493–532.
(27) Brunella, V.; Bracco, P.; Carpentieri, I.; Paganini, M. C.; Zanetti, M.; Costa, L. *Polym. Degrad. Stab.* **2007**, *92*, 1498–1503.
(28) Goldman, M.; Gronsky, R.; Ranganathan, R.; Pruitt, L. *Polymer* **1996**, *37*, 2909–2913.
(29) Plonka, A. *J. Polym. Sci., Part B: Polym. Phys.* **1983**, *21*, 1011–1016.